EDGE ARTICLE

Electrostatic control of regioselectivity *via* ion pairing in a Au(I)-catalyzed rearrangement†

Vivian M. Lau, Craig F. Gorin and Matthew W. Kanan*

The rearrangement of 3-substituted aryl alkynyl sulfoxides catalyzed by cationic Au(I) complexes was studied with different counterions in solvents spanning a range of dielectric constants (ε). Pulsed-gradient diffusion NMR experiments demonstrated strong ion pairing in low-ε solvents. The regioselectivity of the reaction was insensitive to ε when ion pairing was weak but increased monotonically as ε was decreased in the regime of strong ion pairing. DFT calculations of putative product-determining transition states indicated that the product resulting from the more polar transition state is favored due to electrostatic stabilization in the presence of strong ion pairing.

Introduction

Ion pairing has been widely exploited to control the rate and selectivity of reactions that involve charged species.[1–5] In the strategies that have been developed to date, counterions have been used to promote phase transfer, create new steric and chemical environments, bind weakly to reactive centers, participate directly in chemical reactions, or a combination of the above. Because of its proximity to a reactive species in an ion pair, a counterion could in principle affect the selectivity of a reaction through electrostatic interactions that differentiate competing transition states. Although the major electrostatic interaction is the charge–charge attraction that holds an ion pair together, transition states that have significantly different charge distributions could be (de)stabilized to different extents by the local electric field generated by a counterion.[6–9] Here we show that ion pairing changes the regioselectivity of a Au(I)-catalyzed aryl alkynyl sulfoxide rearrangement by favoring the product resulting from a more polar transition state through electrostatic interactions.

Results and discussion

Previous studies have shown that Au(I) complexes catalyze a rearrangement of aryl alkynyl sulfoxides to dihydrobenzothiepinones, a transformation that replaces an aryl C–H bond with a C–C bond.[10–12] To study regioselectivity for this reaction, we prepared 3-Cl aryl alkynyl sulfoxide **1a**, for which C–H functionalization can occur at either the 2- or 6-position.

Department of Chemistry, Stanford University, 337 Campus Drive, Stanford, California 94305, USA. E-mail: mkanan@stanford.edu

† Electronic supplementary information (ESI) available: Experimental details, tables and figures, characterization data. CCDC 1013545. For ESI and crystallographic data in CIF or other electronic format see DOI: 10.1039/c4sc02058h

We first assessed the effects of ligand structure on selectivity using a series of common phosphine (R_3P) and *N*-heterocyclic carbene (NHC) ligands (Table 1). **1a** was reacted with 2 mol% R_3PAuCl or NHCAuCl precatalyst and 2 mol% $NaBAr_4^F$ ($Ar^F = 3,5-(CF_3)_2C_6H_3$) in CH_2Cl_2 at room temperature for 17 h. $NaBAr_4^F$ serves as a Cl^- abstractor to generate an active cationic $R_3PAu(I)$ or NHCAu(I) catalyst. These conditions gave clean conversion to the two expected regioisomeric products **2a** and

Table 1 Ligand influence on regioselectivity

Entry	Catalyst (2 mol%)	3a : 2a[a]	Yield[b] (%)
1	**IMes**AuCl/$NaBAr_4^F$	0.7 : 1	46
2	**IPr**AuCl/$NaBAr_4^F$	1.3 : 1	32
3	**SIPr**AuCl/$NaBAr_4^F$	1.9 : 1	78
4	**Ph₃P**AuCl/$NaBAr_4^F$	0.6 : 1	25
5	(**o-tol**)₃PAuCl/$NaBAr_4^F$	0.6 : 1	30
6	**SPhos**AuCl/$NaBAr_4^F$	0.6 : 1	32
7	**XPhos**AuCl/$NaBAr_4^F$	0.6 : 1	46

IMes: Ar = 2,4,6-Me₃C₆H₂
IPr: Ar = 2,6-*i*Pr₂C₆H₃
SIPr: Ar = 2,6-*i*Pr₂C₆H₃, saturated

SPhos: R₁ = OMe, R₂ = H
XPhos: R₁ = R₂ = *i*Pr

[a] Determined by NMR of crude reaction mixture. [b] Determined by NMR using an internal standard.

3a in moderate to good yields and recovery of the starting material. For NHCAu(ɪ) catalysts, increasing the steric demand of the NHC (**IMes** < **IPr** < **SIPr**)[13] increased the **3a** : **2a** ratio from 0.7 : 1.0 to 1.9 : 1.0, favoring functionalization at the more accessible C–H bond (Table 1, entries 1–3). For the R$_3$PAu(ɪ) catalysts with R$_3$P = **Ph$_3$P**, **(o-tol)$_3$P**, **SPhos**, or **XPhos**, the selectivity was completely insensitive to ligand structure. The ratio of **3a** : **2a** was 0.6 : 1.0 with all of these catalysts despite their substantially different steric and electronic properties (Table 1, entries 4–7).[13] Overall, the ligand screen highlights the difficulty of controlling regioselectivity for this aryl C–H functionalization by changing the ligand structure.

To test whether ion pairing could affect selectivity, we performed the reaction with different counterions in solvents that span a range of dielectric constants (ε). Nitrile complexes [NHCAu(NCR)]X and [R$_3$PAu(NCR)]X (X = anion) were used as pre-catalysts in these experiments to obviate Cl$^-$ abstraction. Spontaneous dissociation of NCR generates the catalytically active cationic Au(ɪ) complex. The reactions were performed with 2.5 mM **1a** and 2 mol% catalyst loading at room temperature. The reactions were stopped after 4 h to determine the product ratio using ^{1}H NMR. Unoptimized yields varied from 17% to 88% depending on the ligand (Table S3 and S4†). Recovered substrate **1a** accounted for essentially all of the remaining material.

The dielectric constant of the solvent affected the regioselectivity obtained with each of the Au(ɪ)-catalysts in a counterion-dependent manner. The results for NHCAu(ɪ) complexes are shown in Fig. 1a. With [IPrAu(NCPh)]BAr$_4^{\text{F}}$, the solvent had little effect on selectivity. The **3a** : **2a** ratio ranged from 0.8 : 1.0 to 1.2 : 1.0 across seven solvents with ε ranging from 2.4 (toluene) to 20.7 (acetone). With [IPrAu(NCMe)]SbF$_6$, however, a significant solvent dependence was observed. For solvents with $\varepsilon \geq 8.9$ (CH$_2$Cl$_2$, (CH$_2$Cl)$_2$, acetone), the **3a** : **2a** ratio was similar to the ratio with the BAr$_4^{\text{F}-}$ complex. For solvents with $\varepsilon \leq 6.0$, the ratio increased monotonically as ε decreased, reaching 2.7 : 1.0 in toluene. The same trend was observed with [IPrAu(NCMe)]BF$_4$, but the increase in the ratio for $\varepsilon \leq 6.0$ was attenuated. Thus, the counterion determined the dependence of the selectivity on ε, with the magnitude given by the order SbF$_6^- >$ BF$_4^- >$ BAr$_4^{\text{F}-} \approx 0$. The same solvent and counterion dependencies were observed with the **IMes** and **SIPr** complexes (Fig. 1a and Table S2†). These effects added to the effects of the steric properties of the ligand such that the largest **3a** : **2a** ratio, 4.5 : 1.0, was obtained with [SIPrAu(NCMe)]SbF$_6$ in toluene.

Larger counterion-dependent responses to ε were obtained with phosphine complexes. Since BAr$_4^{\text{F}-}$ complexes proved to be unstable in solution, we compared complexes with SbF$_6^-$, PF$_6^-$, and BF$_4^-$ counterions. The same trends were observed in all cases: the **3a** : **2a** showed essentially no dependence on ε for solvents with an $\varepsilon > 8$, but increased monotonically as ε was decreased below 8 (Fig. 1b). The changes were significantly larger with SbF$_6^-$ than with PF$_6^-$ or BF$_4^-$ and they varied with
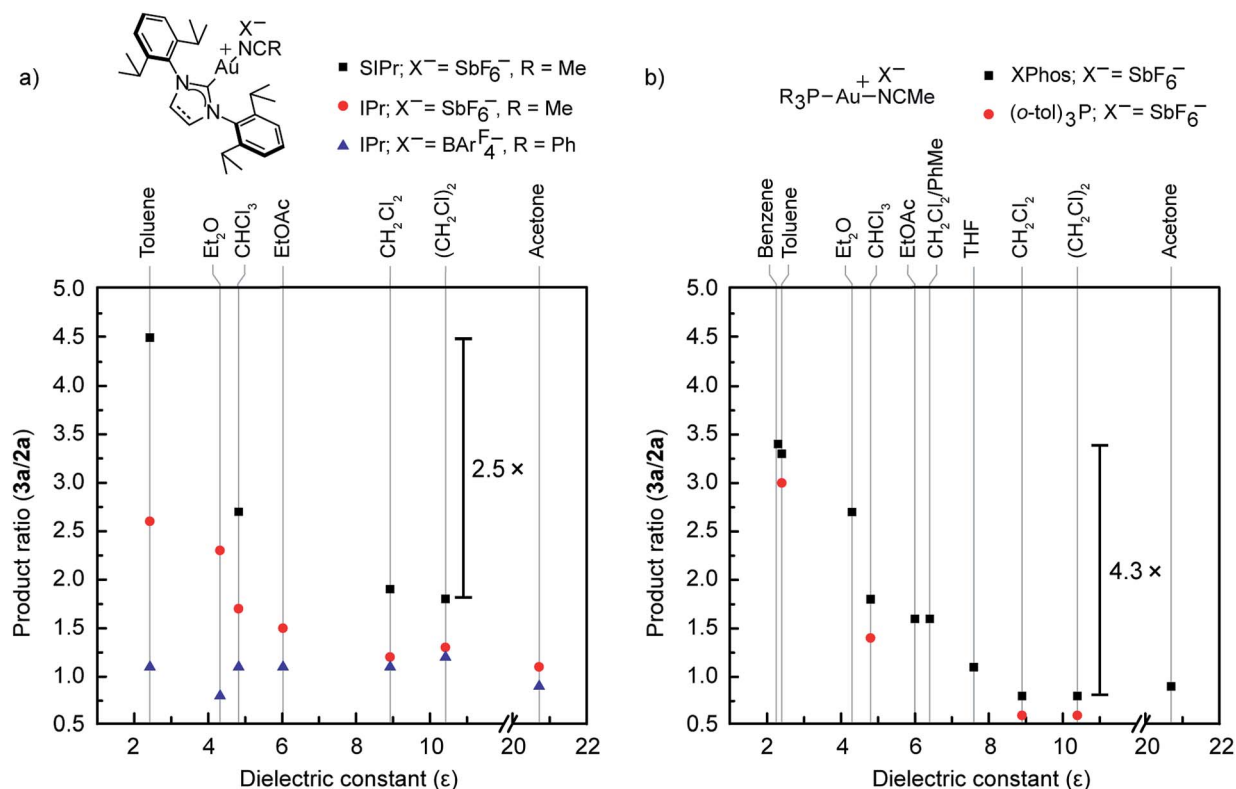

Fig. 1 Effect of solvent dielectric on product ratio for substrate **1a**, catalyzed by [NHCAu(NCR)]X (a) and [R$_3$PAu(NCMe)]X (b). Magnitude of the dielectric response is dependent on the ligand and identity of counterion X$^-$.

the phosphine structure in the order **XPhos** $\approx$ **(o-tol)$_3$P** > **Ph$_3$P** (Table S2†). With **XPhos** and **(o-tol)$_3$P** ligands and SbF$_6^-$ counterion, the **3a** : **2a** ratio increased by a factor of 4.3–5.0 in going from ε = 8.9 (CH$_2$Cl$_2$) to ε = 2.4 (toluene). Only the solvent's ε impacted selectivity and not its molecular properties (dipole moment, coordinating ability, *etc.*) The product ratios obtained in solvent mixtures matched the expected value for their calculated ε.

The dependence of the product ratio on ε and the choice of counterion suggests that the selectivity-determining step proceeds from an ion-paired intermediate in low-ε solvents. Previous diffusion NMR studies of many organometallic complexes have shown that ion pairing is strongly favored in CDCl$_3$ and less polar solvents.[14,15] Weaker, but still substantial, ion pairing has been observed for cationic R$_3$PAu(I) and NHCAu(I) complexes paired with BF$_4^-$ in CD$_2$Cl$_2$.[16–18] To assess the extent of ion pairing for the catalysts used here, we performed pulsed gradient spin echo (PGSE) diffusion ^{1}H NMR measurements using 5 mM solutions of [IPrAu(NCPh)]BAr$_4^F$, and [IPrAu(NCMe)]SbF$_6$ in CD$_2$Cl$_2$ and CDCl$_3$ at 25 °C. The diffusion coefficients (D) of the ions were obtained from Stejskal–Tanner plots (Fig. S1†). To compare between CD$_2$Cl$_2$ and CDCl$_3$, the hydrodynamic radii (r_H) of the ions were calculated using the Stokes–Einstein equation (see ESI†). An increase in the r_H value from one solvent to another indicates an increase in the extent of ion pairing.[14]

^{1}H PGSE NMR measurements of [IPrAu(NCPh)]BAr$_4^F$ yielded an r_H value for the cation that increased from 6.6 Å in CD$_2$Cl$_2$ to 7.2 Å in CDCl$_3$, and an r_H for the anion that increased from 6.6 Å to 7.3 Å (Table 2). Since the molecular radius of [IPrAu(NCPh)]BAr$_4^F$ estimated from the crystallographic cell volume is 7.3 Å,[19] the r_H values in CDCl$_3$ are consistent with complete ion pairing in this solvent. This result also suggests that ion pairing is likely strongly favored in CDCl$_3$ for all complexes studied here because BAr$_4^{F-}$ is larger and much more lipophilic than the other counterions. The smaller r_H values for BArF$_4^-$ and [IPrAu(NCPh)]$^+$ in CD$_2$Cl$_2$ indicate much weaker ion pairing in this solvent. ^{1}H PGSE measurements of additional complexes indicated that the hydrodynamic radii for unpaired [IPrAu(NCPh)]$^+$ and BAr$_4^{F-}$ were ~6.3 Å and ~6.4 Å, respectively (Table S1†). For [IPrAu(NCPh)]SbF$_6$, only the cation r_H values could be obtained because the quadrupole moment of Sb renders the SbF$_6^-$ species ^{19}F NMR-silent. The cation r_H for

this complex increased from 5.8 Å in CD$_2$Cl$_2$ to 6.3 Å in CDCl$_3$, again indicating much stronger ion pairing in CDCl$_3$.

The diffusion NMR results, combined with extensive data from other organometallic complexes,[14,15,17,18] indicates that the equilibria strongly favor the ion paired forms for the NHCAu(I) and R$_3$PAu(I) complexes in CDCl$_3$ and all less polar solvents. The monotonic increase of the **3a** : **2a** ratio as ε is decreased below 8 for all complexes therefore is not likely the result of a significant increase in the extent of ion pairing but instead reflects an increased strength of the effect of the counterion on the product-determining transition states (see below).

To gain further insight into the origin of the ion pairing effect, we explored its dependence on the aryl substituent. Additional 3-substituted aryl alkynyl sulfoxides **1b–1f** were reacted with [(o-tol)$_3$PAu(NCMe)]SbF$_6$ to yield regioisomeric products **2b–2f** and **3b–3f**. Fig. 2 shows the product ratios, **3x** : **2x**, in CH$_2$Cl$_2$, CHCl$_3$, and toluene. The magnitude of the change in product ratio from high ε (CH$_2$Cl$_2$) to low ε (toluene) exhibited a strong dependence on the substituent. Me-substituted **1b** showed essentially no response to the change in ε. For the rest of the substrates, the **3x** : **2x** ratio increased from high ε to low ε, with the magnitude of the change given by the order OMe < Br < F < Cl < CF$_3$ (Table 3). For CF$_3$-substituted **1f**, the ratio increased by a factor of 6.3. In general, a smaller increase was obtained in CHCl$_3$ compared to toluene, consistent with the trend evident in Fig. 1.

The absence of a correlation between the size of the substituent and the magnitude of the selectivity change from high-ε to low-ε solvent indicates that ion pairing does not principally affect selectivity *via* steric interaction. The results in Fig. 1 and 2 instead implicate an electrostatic effect of the counterion on the energy barriers leading to the two products. To probe electrostatic differences between the reactions with different substrates, DFT calculations were performed for
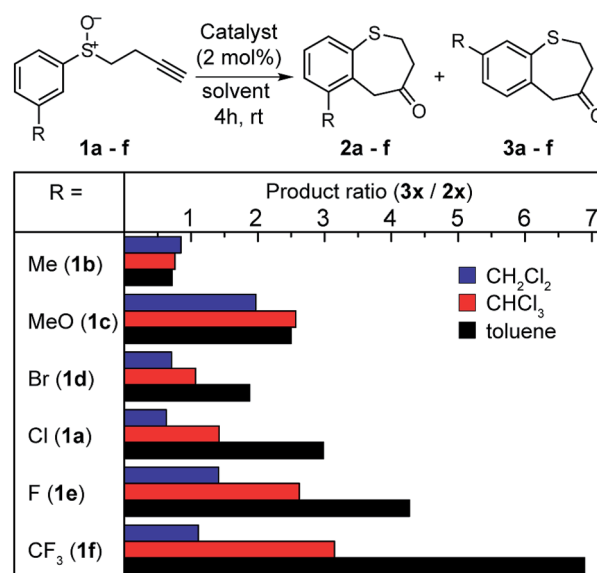

Fig. 2 Substrate-dependent change in regioselectivity in CH$_2$Cl$_2$, CHCl$_3$ and toluene. Catalyst = [(o-tol)$_3$PAu(NCMe)]SbF$_6$.

Table 2 Solvent dependence of the diffusion coefficient D (10^{-10} m^2 s^{-1}) and hydrodynamic radius r_H (Å) of representative Au(I) complexes

Complex	Solvent		D	r_H
[IPrAu(NCPh)]BAr$_4^F$	CDCl$_3$	Cation	6.0	7.2
		Anion	5.9	7.3
	CD$_2$Cl$_2$	Cation	8.7	6.6
		Anion	8.7	6.6
[IPrAu(NCMe)]SbF$_6$	CDCl$_3$	Cation	7.0	6.3
	CD$_2$Cl$_2$	Cation	10.3	5.8

putative product-determining transition states for each substrate. Recent experimental and computational studies provide strong evidence that C–C bond formation occurs through an irreversible [3,3]-sigmatropic rearrangement of a cationic vinyl Au intermediate I (Table 3).[12,20,21] We calculated the [3,3] transition state leading to each regioisomer for the substrates in Fig. 2 with a model Me$_3$P–Au(I) catalyst. We then calculated a dipole moment (ρ) for each transition state using the center of nuclear charge as the origin. Fig. 3 shows the charge density maps for the regioisomeric transition states for substrates **1b** and **1f**. The difference in the magnitude of the dipole moments ($\Delta|\rho|$) indicates the extent to which the transition states differ in their charge distributions. The calculations revealed a strong correlation between $\Delta|\rho|$ and the magnitude of the change in the product ratio upon switching from CH$_2$Cl$_2$ to toluene: $\Delta|\rho| \approx 0$ with CH$_3$-substituted sulfoxide and increased in the order OMe < F < Cl < Br < CF$_3$ (Table 3).

Ion pairing favored the isomer (**3a**, **3c–3f**) that is formed from the more polar product-determining transition state. This result indicates that the paired anion electrostatically stabilizes the transition state leading to the major product to a greater extent than it stabilizes the competing transition state. The strength of the electrostatic interactions that energetically differentiate the two transition states depends on the ε of the medium surrounding the ion pair, which explains why selectivity continues to rise as ε is decreased below 5 even though it is unlikely that the extent of ion pairing changes appreciably in
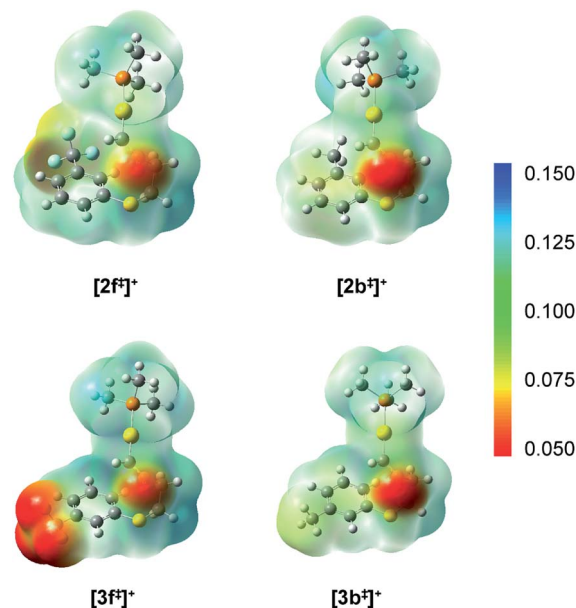

Fig. 3 Charge density maps of the product-determining transition states for substrates with CH$_3$ ([**2b‡**]$^+$, [**3b‡**]$^+$) and CF$_3$ ([**2f‡**]$^+$, [**3f‡**]$^+$) substituents.

this regime. The ion pairing effect is in contrast to the absence of a response to solvent polarity when $\varepsilon \geq 8$. Increasing ε does not significantly favor the pathway proceeding through the more polar transition state whereas ion pairing in a low-ε medium does.

In addition to the substrate, the strength of the ion pairing effect depends on the structure of both the counterion and the ligand. This dependence most likely reflects changes to the placement(s) of the counterion in the ion pair. Maximum electrostatic differentiation of transition states requires placing the counterion as close as possible to the complex and in a position where it can afford the greatest stabilization to the more polar transition state. No effect is seen when pairing with BAr$_4$$^{F-}$ because its large radius places negative charge too far away. The difference between SbF$_6$$^-$ and PF$_6$$^-$ or BF$_4$$^-$ suggests that SbF$_6$$^-$ is better positioned in the ion pair. The relatively small ion pairing effect for Br-substituted **1d** given the large $\Delta|\rho|$ for this substrate may also reflect poor counterion placement. Additional nuclear Overhauser effect NMR studies[17,22,23] and molecular dynamics simulations will be necessary to shed light on these important structural details. Tuning the ligand and counterion structure to adjust ion placement may substantially increase the selectivity afforded by this approach.

Conclusions

In summary, we have demonstrated that ion pairing can control selectivity by preferentially stabilizing more polar transition states. This strategy may be applicable to diverse synthetic challenges because many reactions involve competing pathways with significantly different charge distributions.

Table 3 Calculated dipole moments of isomeric transition states leading to products **2x** and **3x**

R =	ρ (**2x‡**) (D)	ρ (**3x‡**) (D)	$\Delta|\rho|$ (D)	$\dfrac{P_{\text{toluene}}}{P_{\text{CH}_2\text{Cl}_2}}$[a]
Me (**1b**)	4.1	4.0	−0.1	0.9
MeO (**1c**)	2.9	4.8	0.7	1.3
F (**1e**)	2.6	5.4	2.5	3.1
Cl (**1a**)	2.5	5.9	3.3	5.0
Br (**1d**)	2.4	7.5	5.0	2.7
CF$_3$ (**1f**)		9.0	6.6	6.3

[a] P_{toluene} and $P_{\text{CH}_2\text{Cl}_2}$ are the product ratios (**3x**/**2x**) in toluene and CH$_2$Cl$_2$.

Acknowledgements

Notes and references

1 C. M. Starks, C. L. Liotta and M. Halpern, *Phase-Transfer Catalysis*, Chapman & Hall, New York, NY, 1994.

2 M. Delferro and T. J. Marks, *Chem. Rev.*, 2011, **111**, 2450–2485.

3 S. E. Denmark, N. D. Gould and L. M. Wolf, *J. Org. Chem.*, 2011, **76**, 4337–4357.

4 K. Brak and E. N. Jacobsen, *Angew. Chem., Int. Ed.*, 2013, **52**, 534–561.

5 M. Mahlau and B. List, *Angew. Chem., Int. Ed.*, 2013, **52**, 518–533.

6 A. Warshel, P. K. Sharma, M. Kato, Y. Xiang, H. B. Liu and M. H. M. Olsson, *Chem. Rev.*, 2006, **106**, 3210–3235.

7 S. G. Boxer, *J. Phys. Chem. B*, 2009, **113**, 2972–2983.

8 C. F. Gorin, E. S. Beh and M. W. Kanan, *J. Am. Chem. Soc.*, 2012, **134**, 186–189.

9 C. F. Gorin, E. S. Beh, Q. M. Bui, G. R. Dick and M. W. Kanan, *J. Am. Chem. Soc.*, 2013, **135**, 11257–11265.

10 N. D. Shapiro and F. D. Toste, *J. Am. Chem. Soc.*, 2007, **129**, 4160–4161.

11 G. T. Li and L. M. Zhang, *Angew. Chem., Int. Ed.*, 2007, **46**, 5156–5159.

12 B. Lu, Y. X. Li, Y. L. Wang, D. H. Aue, Y. D. Luo and L. M. Zhang, *J. Am. Chem. Soc.*, 2013, **135**, 8512–8524.

13 H. Clavier and S. P. Nolan, *Chem. Commun.*, 2010, **46**, 841–861.

14 A. Macchioni, G. Ciancaleoni, C. Zuccaccia and D. Zuccaccia, *Chem. Soc. Rev.*, 2008, **37**, 479–489.

15 P. S. Pregosin, P. G. A. Kumar and I. Fernandez, *Chem. Rev.*, 2005, **105**, 2977–2998.

16 P. S. Pregosin, *Prog. Nucl. Magn. Reson. Spectrosc.*, 2006, **49**, 261–288.

17 D. Zuccaccia, L. Belpassi, F. Tarantelli and A. Macchioni, *J. Am. Chem. Soc.*, 2009, **131**, 3170–3171.

18 G. Ciancaleoni, L. Belpassi, F. Tarantelli, D. Zuccaccia and A. Macchioni, *Dalton Trans.*, 2013, **42**, 4122–4131.

19 N. Huguet, D. Leboeuf and A. M. Echavarren, *Chem.–Eur. J.*, 2013, **19**, 6581–6585.

20 A. B. Cuenca, S. Montserrat, K. M. Hossain, G. Mancha, A. Lledos, M. Medio-Simon, G. Ujaque and G. Asensio, *Org. Lett.*, 2009, **11**, 4906–4909.

21 C. Obradors and A. M. Echavarren, *Chem. Commun.*, 2014, **50**, 16–28.

22 D. Zuccaccia, L. Belpassi, A. Macchioni and F. Tarantelli, *Eur. J. Inorg. Chem.*, 2013, **2013**, 4121–4135.

23 D. Zuccaccia, L. Belpassi, L. Rocchigiani, F. Tarantelli and A. Macchioni, *Inorg. Chem.*, 2010, **49**, 3080–3082.